Electronic Supplementary Material (ESI) for Physical Chemistry Chemical Physics.

Absolute Upconversion Quantum Yields of Blue-emitting $LiYF_4:Yb^{3+},Tm^{3+}$ Upconverting Nanoparticles

Michael S. Meijer,[1] Paola A. Rojas-Gutierrez,[2] Dmitry Busko,[3] Ian A. Howard,[3,4] Florian Frenzel,[5] Christian Würth,[5] Ute Resch-Genger,[5] Bryce S. Richards,[3,4] Andrey Turshatov,[3] John A. Capobianco,[2] Sylvestre Bonnet[1]**

[1]Leiden Institute of Chemistry, Leiden University, Gorlaeus Laboratories, P.O. Box 9502, 2300 RA Leiden, The Netherlands; [2]Department of Chemistry and Biochemistry, and Centre for NanoScience Research, Concordia University, Montreal, Quebec, H4B 1R6, Canada; [3]Institute of Microstructure Technology, Karlsruhe Institute of Technology, Hermann-von-Helmholtz-Platz 1, 76344 Eggenstein-Leopoldshafen, Germany; [4]Light Technology Institute, Karlsruhe Institute of Technology, Engesserstrasse 13, 76131 Karlsruhe, Germany; [5]Federal Institute for Materials Research and Testing (BAM), Division Biophotonics, Richard-Willstätter-Straße 11, 12489 Berlin, Germany.

Corresponding authors: bonnet@chem.leidenuniv.nl, john.capobianco@concordia.ca

SUPPORTING INFORMATION

Table of Contents

1. Nanoparticle synthesis

1.1. Materials and general methods

Thulium oxide (Tm_2O_3, 99.99+ %), ytterbium oxide (Yb_2O_3, 99.99%), yttrium oxide (Y_2O_3, 99.99+ %), trifluoroacetic acid (CF_3COOH, 99%), lithium trifluoroacetate (CF_3COOLi, 98%), oleic acid (technical grade, 90%), and 1-octadecene (technical grade, 90%) were all purchased from Sigma-Aldrich and were used without further purification. All other solvents were obtained from major chemical suppliers and used as received.

1.2. Synthesis of LiYF4:Yb^{3+},Tm^{3+} upconverting nanoparticles

$LiYF_4$:Tm^{3+},Yb^{3+} UCNPs were synthesized *via* thermal decomposition, which was comprised of a two-step process.[1,2] In the first step, a mixture of water/trifluoroacetic acid (10 mL, 1:1) was added to a 3-neck round-bottom flask containing Tm_2O_3 (0.0024 g, 6.25×10^{-6} mol, 0.5 mol% Tm^{3+}), Yb_2O_3 (0.1232 g, 3.13×10^{-4} mol, 25 mol% Yb^{3+}), and Y_2O_3 (0.2103 g, 9.31×10^{-4} mol). The cloudy solution was heated (80 °C) under reflux until it was clear. The resulting solution was then dried at 60 °C to form the trifluoroacetate lanthanide precursors. In the second step, CF_3COOLi

(0.2999 g, 2.50×10^{-3} mol) was added to the dried precursor solids along with oleic acid (20 mL) and 1-octadecene (20 mL) and the mixture was degassed for 30 min at 120 °C. The temperature was increased at a rate of 10 °C·min^{-1} to 315 °C under an argon atmosphere. The reaction mixture was maintained at 315 °C under stirring for 60 min and under an argon atmosphere. After cooling to room temperature, absolute ethanol was added to the reaction mixture to precipitate the $LiYF_4$:Tm^{3+},Yb^{3+} UCNPs, which were subsequently isolated *via* centrifugation (3000 rpm, 15 min). The pellet was washed with a 1:3 hexane/ethanol mixture twice to remove any impurities. After purification, the sample was stored and shipped as a solid under a layer of ethanol.

1.3. Synthesis of $LiYF_4$ undoped nanoparticles

$LiYF_4$ undoped nanoparticles were synthesized by the same method as described for the doped nanoparticles in section 1.2, using only Y_2O_3 (0.2103 g, 9.31×10^{-4} mol) in the first step to form the yttrium trifluoroacetate precursor instead of a mixture with thulium and ytterbium oxides. The second step of the synthesis was followed as described in section 1.2.

2. Nanoparticle characterization

2.1. Powder X-ray diffraction (PXRD)

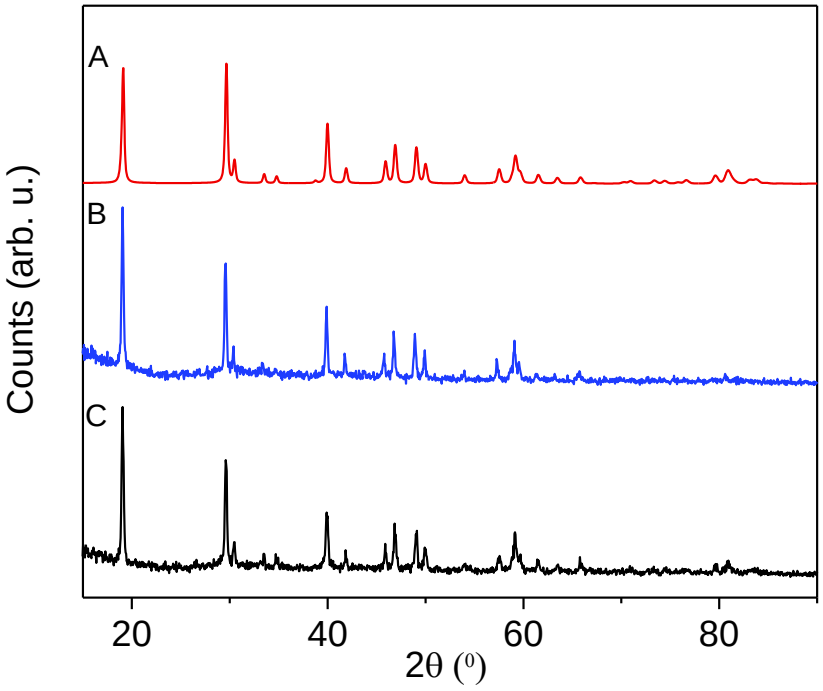

Figure S1. X-ray powder diffraction analysis of (A) calculated line pattern for tetragonal $LiYF_4$ shown for reference (JCPDS 81-2254), (B) undoped oleate capped $LiYF_4$ nanocrystals and (C) oleate-capped $LiYF_4$:Tm^{3+},Yb^{3+}nanocrystals.

Figure S1 shows the X-Ray power diffraction (XRPD) of the oleate-capped $LiYF_4$:Tm^{3+},Yb^{3+} UCNPs, undoped oleate-capped $LiYF_4$ UCNPs and the calculated standard of the JCPDS pattern. The peak positions correspond to the reported pattern of tetragonal $LiYF_4$ (JCPDS no. 81-2254). The patterns for both doped and undoped $LiYF_4$ nanoparticles were collected at room temperature using a Bruker D2 Phaser XRD System equipped with a LYNXEYE one-dimensional X-ray diffraction detector, based on Bruker AXS' compound silicon strip technology. Scan range was set

from 15 – 90° 2θ with a step size of 0.5° and a count time of 1 s. A PMMA background insert disk was used as sample holder.

2.2. Transmission electron microscopy (TEM) and size distribution

Transmission electron microscopy (TEM) was used to evaluate the morphology and particle size distribution (PSD) of the prepared nanoparticles. 300 particles of doped and undoped nanoparticles were evaluated to obtain the size distribution. The oleate-capped $LiYF_4:Tm^{3+},Yb^{3+}$ UCNPs showed a diamond-like morphology with an average size of 87 nm (± 9 nm) long diagonal length and a small diagonal length of 50 nm (± 4 nm). The oleate-capped $LiYF_4$ NPs showed a diamond-like morphology with an average size of 87 nm (± 6 nm) long diagonal length and a small diagonal length of 48 nm (± 3.5 nm). The micrographs were collected using a Jeol JEM-2100F microscope operating at 120 kV capable of imaging resolution of 0.1 nm. Samples were prepared by dropping sample solutions (1 $mg.mL^{-1}$ in toluene) onto a 300-mesh Formvar/carbon coated copper grid (3 mm in diameter) followed by the evaporation of the solvent.

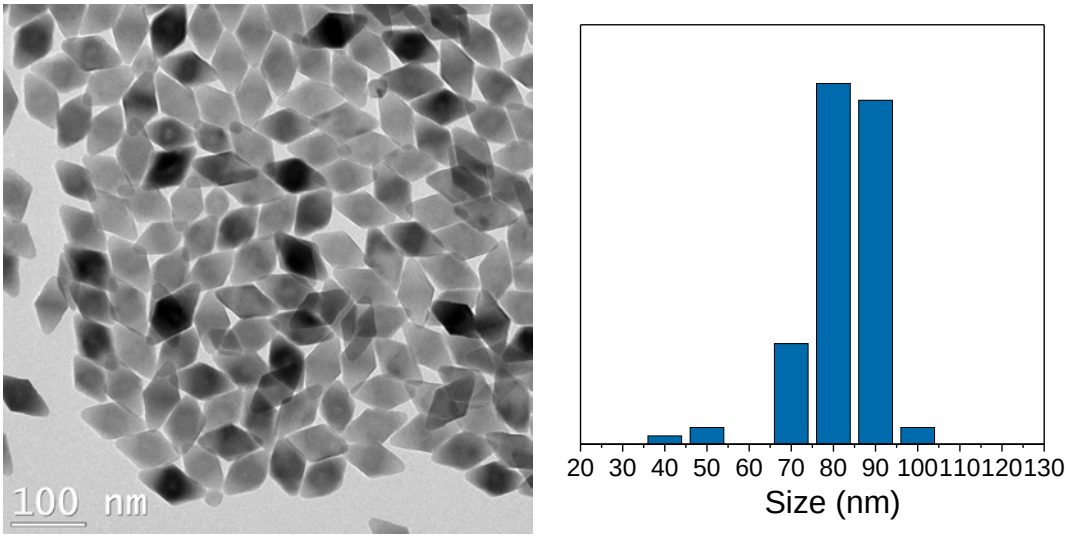

Figure S2. Transmission electron micrograph (left) of oleate-capped $LiYF_4:Tm^{3+},Yb^{3+}$ UCNPs (1 $mg{\cdot}ml^{-1}$ in toluene). Histogram (right) of the particle size distribution obtained with respect to the long diagonal 87 ± 9 nm from the TEM images (average of ~ 300 nanocrystals).

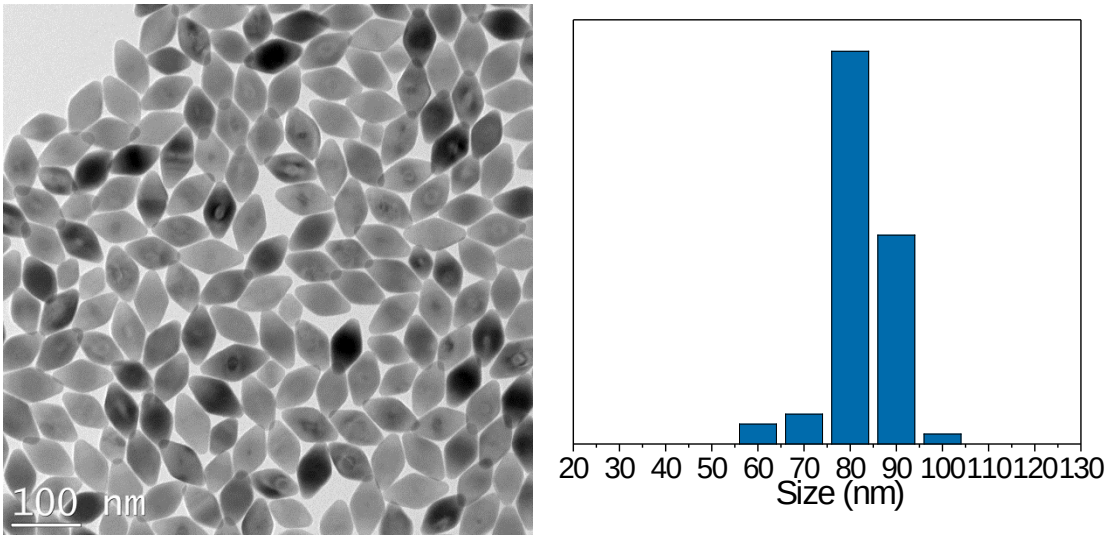

Figure S3. Transmission electron micrograph (left) of undoped oleate-capped $LiYF_4$ UCNPs (1 mg·ml^{-1} in toluene). Histogram (right) of the particle size distribution obtained with respect to the long diagonal 87 ± 6 nm from the TEM images (average of ~ 300 nanocrystals).

3. Absolute quantum yield determination using the Leiden setup

3.1. Experimental setup

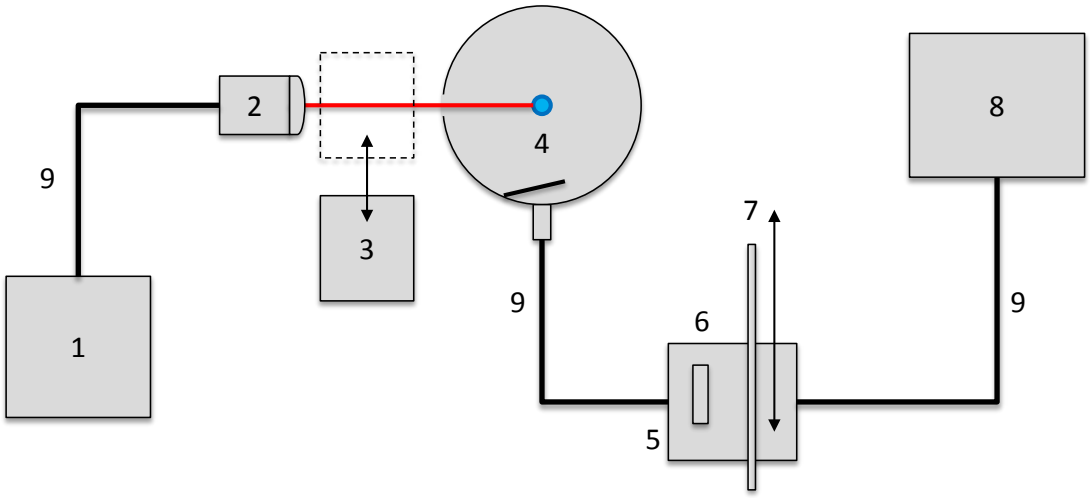

Scheme S1. Setup used for absolute quantum yield measurements. (1) laser source, (2) collimating lens, mechanical iris and focusing lenses, (3) power meter (adjustable in position), (4) integrating sphere with sample tube in the center, (5) filter holder, (6) 875-nm short pass filter that can be installed or removed, (7) variable neutral density filter that can be installed or removed, (8) CCD spectrometer, (9) optical fibers.

The integrating sphere setup used for determining the quantum yield of upconversion in Leiden in depicted in Scheme S1. The excitation source was a fiber-coupled CW 969-nm diode laser (MDL-H-980-3W, CNI Laser, Changchun, China), coupled into a 200-µm multimode optical fiber, leading to a collimating lens (F220SMA-980, Thorlabs). After collimation, the light passed a mechanical iris, and two lenses (f = 10 and 5 cm) to produce a ca. 2 mm beam (*vide infra*) with 200 mW optical power (P_{exc} = 5.0 W·cm^{-2}). The excitation power was measured using a S310C thermal sensor

connected to a PM100USB power meter (Thorlabs). A PTFE-coated AvaSphere-30-IRRAD integrating sphere (30 mm diameter, reflectance > 98%), fitted with three ports (entry, exit and sample port), and an AvaSpec-ULS2048L StarLine CCD spectrometer were obtained from Avantes (Apeldoorn, The Netherlands). The integrating sphere and spectrometer were calibrated together using an Avalight-HAL-CAL-ISP30 NIST traceable calibration lamp from Avantes (9.5% relative uncertainty vs. NIST standard), so that the observed intensities are expressed as a photon flux (mol photons·s^{-1}·m^{-2}). The filter holder was fabricated by our own mechanical department, and held a NDL-25C-4 variable neutral density filter (Thorlabs) or an OD4 875 nm short pass filter (Edmund Optics, York, United Kingdom, part no. 86-106, $T_{430\text{-}860\ nm} \approx 97.3 \pm 1.3\%$). An Avalight-DHc (Avantes) deuterium-halogen lamp was used as a white light source for the determination of the transmission functions of the filters used. The spectra were recorded with Avasoft 8.5 software from Avantes, and further processed with Microsoft Office Excel 2010 and Origin Pro 9.1 software.

3.2. Quantum yield calculation method

The upconversion photoluminescence quantum yield (Φ_{UC}) is defined by Equation S1:

$$\Phi_{UC} = \frac{number\ of\ upconverted\ photons}{number\ of\ low\text{-}energy\ photons\ absorbed} = \frac{q_{p\text{-}em}}{q_{p\text{-}abs}} \qquad \textbf{Equation S1}$$

Here, $q_{p\text{-}em}$ is the upconverted emission photon flux (in photons·s^{-1}) and $q_{p\text{-}abs}$ is the photon flux absorbed by the sensitizer species (in photons·s^{-1}).

Φ_{UC} can be calculated by Equation S2:

$$\Phi_{UC} = \frac{\int_{\lambda_1}^{\lambda_2} I_{UC}(\lambda) d\lambda}{q_{p\text{-}abs}} \qquad \textbf{Equation S2}$$

Here, $I_{UC}(\lambda)$ is the spectral luminescence intensity (in photons·s^{-1}·nm^{-1}), and λ_1 and λ_2 are the low- and high-wavelength boundaries, respectively, of either the entire upconverted emission spectrum, or the 4f-4f transition of interest. $q_{p\text{-}abs}$ is determined by subtracting the spectral light intensity of the excitation source that has passed through the sample ($I_{exc\text{-}sample}$, in photons·s^{-1}·nm^{-1}) from the spectral light intensity of the excitation source that has passed through a blank sample ($I_{exc\text{-}blank}$, in photons·s^{-1}·nm^{-1}), and by integrating over the excitation wavelength range λ_3 to λ_4, see Equation S3. The blank sample consisted of a dispersion of undoped $LiYF_4$ UCNPs of a similar size, dispersed in the same solvent at the same concentration as the sample. Due to the lack of photo-active dopants, it did not absorb at the excitation wavelength.

$$q_{p-abs} = \int_{\lambda_3}^{\lambda_4} (I_{exc\text{-}blank}(\lambda) - I_{exc\text{-}sample}(\lambda)) d\lambda \qquad \textbf{Equation S3}$$

Equation S2 can then be expressed as Equation S4:

$$\Phi_{UC} = \frac{\int_{\lambda_1}^{\lambda_2} I_{UC}(\lambda) d\lambda}{\int_{\lambda_3}^{\lambda_4} (I_{exc\text{-}blank}(\lambda) - I_{exc\text{-}sample}(\lambda)) d\lambda} \qquad \textbf{Equation S4}$$

The spectrometer and the integrating sphere were calibrated so that the observed intensities are directly proportional to the photon flux, i.e. $I(\lambda) \propto [\text{mol of photons} \cdot \text{s}^{-1} \cdot \text{nm}^{-1}]$. Therefore, integrating these values over the relevant wavelength regions directly provided the flux of photons that arrived at the spectrometer.

Because the intensity of the upconverted light is relatively low compared to that of the exciting laser source the absorption and emission of the sample cannot be measured at the same time. In other words, the laser light saturates the spectrometer, which prevents upconversion to be measured simultaneously. To circumvent this problem, the absorption was measured using a neutral density filter with known transmittance (typically $F_{attn} \approx 0.0015$, i.e., ~ 99.85% attenuation). This filter was placed between the integrating sphere and the spectrometer to measure the absorbed photon flux. For the measurement of the upconverted emission, this filter was replaced by an OD4 short pass filter (< 875 nm) to remove the excitation light. The attenuation factor F_{attn} was averaged over the wavelength range of the laser (950–990 nm).

Additionally, the intensity of the upconverted emission measured was corrected for the minimal absorbance of this light by the shortpass filter used. This was performed by dividing the upconversion luminescence intensity by the transmission curve $T(\lambda)$ of the short pass filter in the wavelength range of the upconverted light. As the shortpass filter strongly absorbed light with a wavelength shorter than 430 nm, this prevented the measurement of any ultraviolet emission by this method. The accordingly corrected equation for Φ_{UC} is Equation S5:

$$\Phi_{UC} = \frac{\int_{\lambda_1}^{\lambda_2} \left(\frac{I_{UC}(\lambda)}{T(\lambda)}\right) d\lambda}{\int_{\lambda_3}^{\lambda_4} \frac{I_{exc\text{-}blank}(\lambda) - I_{exc\text{-}sample}\ (\lambda)}{F_{attn}} d\lambda} \equiv \frac{q_{p\text{-}em}}{q_{p\text{-}abs}} \qquad \textbf{Equation S5}$$

3.3. Experimental procedure

For each measurement, two UCNP dispersions (4% w/v in toluene, ~ 500 µL) were prepared and dispersed thoroughly by sonication: one blank sample, containing undoped $LiYF_4$ nanoparticles, and the sample of interest, containing $LiYF_4$:Yb^{3+},Tm^{3+} nanoparticles. An aliquot (50 µL) of each sample was loaded into specially designed measurement tubes that were made of a quartz EPR-tube bottom (± 7 cm length) fused to a NS-14 glass connector (± 2 cm length), at the top of which a septum was adapted. The tube precisely fitted into a hole made in the integrating sphere, and was suspended in the center of the sphere, in the focal point of the excitation laser beam.

The laser diode was allowed to warm up for 10 minutes prior to the experiment to guarantee a stable output. The measurements were always performed in the same order, i.e. (1) absorption measurement of the blank, (2) absorption measurement of the sample, and (3) emission

measurement of the sample. In this way, the neutral density filter is not moved between the measurement of the blank and sample, ensuring equal attenuation of the non-absorbed excitation light for both spectra. Equally, the sample is not moved between the measurement of its absorption and emission. For the absorption measurements, the neutral density filter was placed in the filter, and replaced by the 875 nm shortpass filter for the emission measurement. All three spectra were recorded for a period of 10 minutes and subsequently averaged, in order to correct for minor instabilities (< 1.5%) in the intensity of the incident laser beam. These instabilities are a major contributing factor to the relative uncertainty in the reported quantum yield values. Integration of the emission bands was performed by fitting the emission bands with one or more Gaussian profiles, and integrating the area under these peaks. This treatment allowed deconvolution of the various emission bands, even though the emission data could only be recorded with a spectral resolution of 9 nm (slit size = 200 µm).

4. Relative excitation power dependence of the upconversion quantum yield (Leiden)

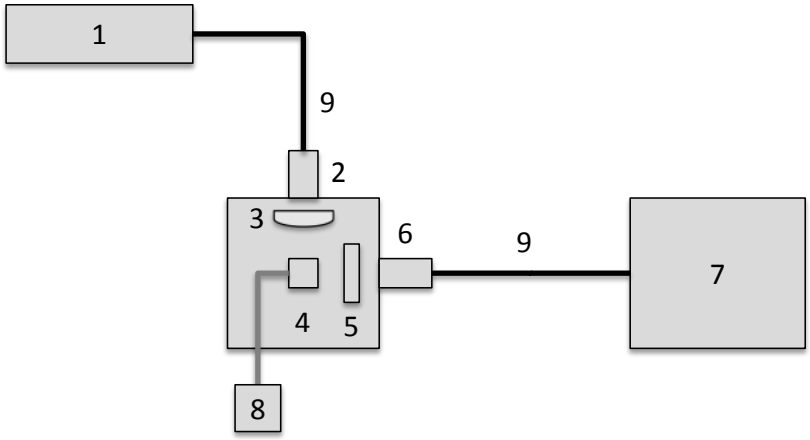

Scheme S2. Setup used for excitation power and temperature dependence measurements. (1) laser source, (2) collimating lens, (3) focusing lenses, (4) temperature-controlled cuvette holder, (5) 875-nm short pass filter, (6) double collimator, (7) CCD spectrometer, (8) thermocouple inserted into the sample, connected to a temperature logger (removed for power dependence measurements), (9) optical fibers.

Power dependence measurements were conducted with a custom-built setup shown in Scheme S2. The excitation source was a fiber-coupled CW 969-nm diode laser (MDL-H-980-3W, CNI Laser, Changchun, China), coupled into a 200-µm multimode optical fiber, leading to a collimating lens (F220SMA-980, Thorlabs, Dachau, Germany). After collimation, the light passed a mechanical iris, and two lenses (f = 10 and 5 cm) to produce a ca. 2 mm beam (*vide infra*). The excitation power was measured using a S310C thermal sensor connected to a PM100USB power meter (Thorlabs). The focused beam passed through the center of a CUV-UV/VIS-TC temperature-controlled cuvette holder (Avantes, Apeldoorn, The Netherlands), typically set to 293.15 K. Temperature control was performed with the use of a TC-125 controller and T-app software from Quantum Northwest (Liberty Lake, WA, USA). The emission spectra were collected at a 90° angle with respect to the excitation beam. The emitted light passed through an OD4 875 nm short pass filter (Edmund Optics, York, United Kingdom, part no. 86-106) and a double collimator into an optical fiber, which led to an AvaSpec-ULS2048L StarLine CCD spectrometer obtained from Avantes. The

spectrometer was calibrated using an Avalight-HAL-CAL-ISP30 NIST traceable calibration lamp from Avantes, so that the observed intensities are expressed as a photon flux (mol photons·s^{-1}).

Direct measurement of the quantum yield of the UCNPs at high excitation powers (> 10 W·cm^{-2}) was prohibited by the instability of the excitation laser, which was observed when the laser diode was used at such excitation powers for the prolonged amounts of time necessary for direct quantum measurements. Therefore, the power dependence of Φ_{UC} was estimated by measuring the upconverted emission in the temperature controlled cuvette holder setup (described above) at a range of power densities between 0.024 and 60 W·cm^{-2}, and scaling Φ_{UC} at 5.0 W·cm^{-2} with the ratio of the upconverted emission at P_{exc} = 5.0 W·cm^{-2} and the P_{exc} of interest by using Equation S6:

$$\Phi_{UC}^{P} = \Phi_{UC}^{5.0\,W/cm2} * \frac{\int_{\lambda_1}^{\lambda_2} I_{UC}^{Pexc}(\lambda)d\lambda}{\int_{\lambda_1}^{\lambda_2} I_{UC}^{5.0\,W/cm2}(\lambda)d\lambda} \qquad \textbf{Equation S6}$$

The sample used for direct quantum yield measurements was diluted to a concentration of 10 mg·mL^{-1} in toluene. About 500 µL of this dispersion were placed in a 104F-QS semi-micro cuvette (Hellma Analytics, Müllheim, Germany). The cuvette was placed in the temperature-controlled cuvette holder and allowed to equilibrate for at least 2 minutes prior to starting the first measurement. Integration of the emission bands was performed by fitting the emission bands with one or more Gaussian profiles, and integrating the area under these peaks. This treatment allowed deconvolution of the various emission bands, even though the emission data could only be recorded with a spectral resolution of 9 nm (slit size = 200 µm).

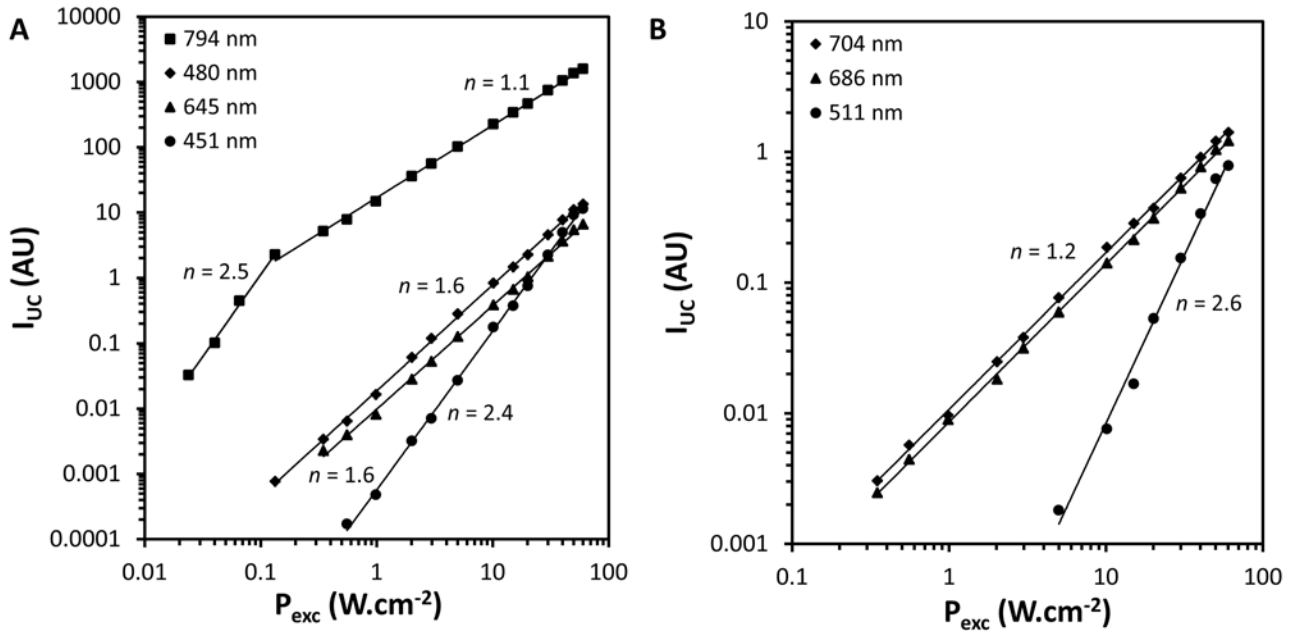

Figure S4. Excitation power dependence of the upconverted emission intensity I_{UC}, for the (a) major and (b) minor thulium emission bands in $LiYF_4$:Yb,Tm UCNPs in toluene as measured on the Leiden setup; λ_{exc} = 969 nm, T = 293 K, [UCNP] = 10 mg·mL^{-1}.

5. Leiden setup beam profiling

A beam profiler was used for measuring the beam diameters of the laser beams in the aforementioned setups and calculating the excitation power densities in $W.cm^{-2}$. The beam profiler consisted of a Trust Webcam Spotlight Pro, of which the front lens was pried off and replaced by NE510A (OD = 1) and NE520A (OD = 2) absorptive neutral density filters (Thorlabs). The focused laser beam, further attenuated using a variable neutral density filter (OD ≈ 2.8, NDL-25C-4, Thorlabs), was pointed directly on the photovoltaic chip of the webcam (4.80 mm wide and 3.60 mm high). Then, $1/e^2$ laser beam diameters in pixels were determined by Beams, an open source beam profiling software downloadable from http://ptomato.name/opensource/beams/beams.html. The beam diameter in millimeters was calculated by dividing the average beam diameter in pixels by the total number of horizontal pixels and multiplying this with the chip width (4.80 mm). Figure S5 depicts an example output of the Beams software, in which the beam diameter of the laser beam was $\frac{277\text{ px}}{640\text{ px}} \times 4.80\text{ mm} = 2.08\text{ mm}$.

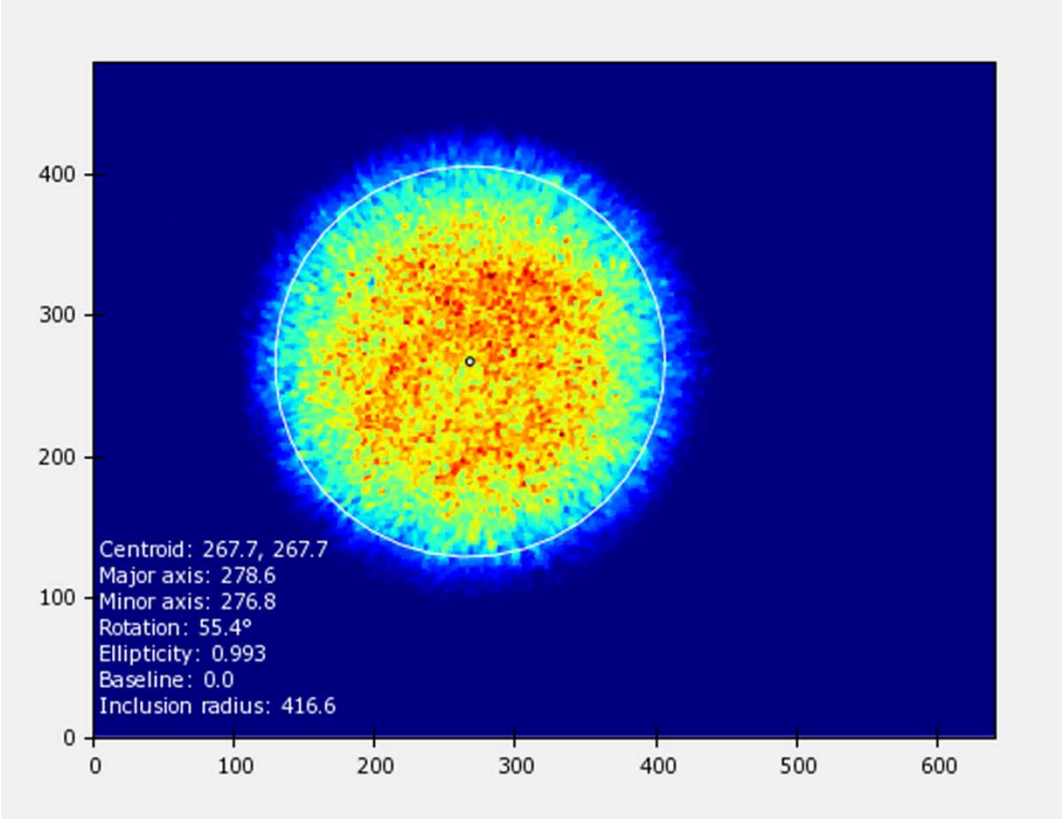

Figure S5. Leiden laser beam diameter (λ_{exc} = 969 nm) visualized by the beam profiling setup in combination with the Beams software package. Axes represent chip width and height in pixels. Colors represent light intensity in increasing order from blue to red.

6. Absolute upconversion quantum yield determination using the Karlsruhe setup

A CW 980 nm laser diode (L980P200, Thorlabs), mounted in a temperature stabilized mount (TCLDM9, Thorlabs) and driven by a laser diode controller (ITC4001, Thorlabs) was focused by a lens (focal length = 75 cm) and directed into an integrating sphere (Labsphere) with a diameter of 150 mm. The beam size on the sample, filled in a quartz cuvette with 5 mm optical path (Hellma Analytics), was measured with a scanning slit optical beam profiler (BP209, Thorlabs) to be equal to 0.9 × 1.3 mm (4σ). An optical fiber with a diameter of 1 mm (FP1000URT, Thorlabs) was used for the collection of the emission from the integrating sphere and to transfer this to the spectrometer (CCS200, Thorlabs). During the absorption measurement (measurement of the laser for direct and indirect excitation of the sample and empty sphere), short integration times, usually 20–50 times shorter than for UC detection, were used. All raw detected spectra were recalculated to give power spectra using an integration time value. The linearity of the signal versus the integration time of the CCD was controlled experimentally. The spectral response of the whole detection system was calibrated using a calibration lamp (HL-3plus-INT-CAL, Ocean Optics) and the correction was further applied to the power spectra. UCNP dispersions were prepared in a manner similar to described in the previous Section 3.3 by the Leiden group.

The quantum yield of upconversion (Φ_{UC}) was calculated according to the 3M procedure described in literature.[3,4] The formula for the calculation is given in Equation S7:

$$\Phi_{UC} = \frac{PD - PI \cdot (1 - A)}{A \cdot ES} \qquad \textbf{Equation S7}$$

where *PD* is the intensity of “photoluminescence direct” for the sample directly excited with the incident beam, *PI* is the intensity of “photoluminescence indirect”, i.e. emission, caused by the diffusively reflected excitation radiation, first hitting the internal wall of the integrating sphere and then the sample, *ES* is the intensity measured for the “empty sphere” (without a sample). *A* is the absorption of the sample, which is calculated according to Equation S8:

$$A = 1 - {}^{LD}/_{LI} \qquad \textbf{Equation S8}$$

Here, *LD* is the “laser direct” – intensity of the excitation source for direct excitation of the sample, and *LI* is the “laser indirect” – intensity of the excitation source for indirect excitation. The values are calculated from the measured spectral fluxes using Equation S9 and S10:

$$PD, PI = \int_{\lambda_1}^{\lambda_2} I_{PD,PI}(\lambda) d\lambda \qquad \textbf{Equation S9}$$

$$ES, LD, LI = \int_{\lambda_3}^{\lambda_4} I_{ES,LD,LI}(\lambda) d\lambda \qquad \textbf{Equation S10}$$

Here, λ_1 and λ_2 (and λ_3 and λ_4) are the low- and high-wavelength boundaries used for integration, respectively, of either the entire UC emission spectrum, or the excitation beam spectral profile.
Because of the nonlinear intensity response of UC, the low absorption of the sample and a relatively low efficiency of UC, the PI is negligible for most of UC samples and is usually neglected for the subsequent calculations, simplifying the formula to:

$$\Phi_{UC} = \frac{PD}{A \cdot ES} \qquad \textbf{Equation S11}$$

7. Absolute upconversion quantum yield determination using the Berlin setup

The measurement procedure and the technical details of the homebuilt integrating sphere setup, which was used for the absolute quantum yield measurements done in Berlin have been previously described in M. Kaiser et al.[5] Briefly, P_{exc}-dependent Φ_{UC} values were obtained absolutely with an existing custom designed integrating sphere setup,[6] modified to meet the requirements of UC luminescence measurements. Its main parts are a highly stable 8 W 976 nm laser diode (wavelength stability < 0.3 nm, power stability < 0.1 %), collimating and focusing optics, and a laser clean filter, which is coupled via a 200 µm-sized optical fiber into a $BaSO_4$-coated integrating sphere (diameter of 15 cm) equipped with a Si-CCD detection system. The intensity-weighted average emission wavelength of the laser diode was adjusted to match the Yb^{3+} absorption peak at 976.4 nm. To realize different beam profiles, lenses with focal lengths of 500 mm and 125 mm were integrated into the excitation light path, yielding a top-hat and a nearly Gaussian beam profile, respectively. For the measurements provided here, a top-hat beam profile was used. To enable precise tuning of the average P_{exc} for both beam shapes, two automated filter wheels equipped with reflective neutral density (ND) filters of known transmittance were placed between the laser diode and the integrating sphere.

Calibration of the integration sphere setup included calibration of the wavelength scale and range of linearity of the detection system following previously described procedures,[6-8] The wavelength-dependent spectral responsivity of the detection channel, including the integrating sphere, optical fiber, monochromator, and detector were characterized with a calibrated spectral radiance transfer standard (calibrated by the Physikalisch-Technische Bundesanstalt (PTB)) from 350–1050 nm using different bandpass filters. The spectral radiance transfer standard consists of a halogen lamp mounted inside an integrating sphere to guarantee a diffuse spectral radiance (Gigahertz-Optik GmbH). The reliability of the emission correction curve was controlled with the aid of the BAM spectral emission standards F003–F005.[9] The excitation beam profile reaching the sample and its power density were determined with a calibrated power meter (Gentec UP19K-1SS-H5-00).

Φ_{UC} was obtained from the directly measured number of emitted photons per number of absorbed photons at different P_{exc} considering solely emitted photons with λ < 900 nm (integration over all UC emission bands between 370 and 890 nm). For the detection of the scattered excitation light

required for calculating the number of absorbed photons in Equation S1, the intense laser light was attenuated with an absorptive ND filter (attenuation factor of ca. 5600) to prevent detector saturation. With these filters, a P_{exc} range of 2 to 425 W·cm^{-2} can be covered for these UCNPs dispersed in toluene. For the determination of the incident photon flux mandatory for the calculation of the number of absorbed photons, the solvent employed for the UCNP dispersion was used as a blank. The absorption of the UCNP samples in toluene was about 2% at the excitation wavelength of 980 nm. For the evaluation of the P_{exc}-dependent Φ_{UC}, the emission intensities I_{UC} (λ_{em}, P_{exc}) and the slope factors $n(P_{exc})$, we chose the following spectral regions: $^1D_2 \rightarrow {}^3F_4$: 433–462 nm, $^1G_4 \rightarrow {}^3H_6$: 462–500 nm, $^1I_6 \rightarrow {}^3F_3$: 505–516 nm, $^1G_4 \rightarrow {}^3F_4$: 610–675 nm, $^3F_2 \rightarrow {}^3H_6$: 675–720 nm, $^3F_3 \rightarrow {}^3H_6$: 675–720 nm and $^3H_4 \rightarrow {}^3H_6$: 720–890 nm. To obtain the number of emitted photons, the measured blank and spectrally corrected luminescence spectra/intensity values and spectral UC intensities were multiplied with λ/hc_0 to obtain spectral photon fluxes (s^{-1}·m^{-3}) and luminescence quantum yields.

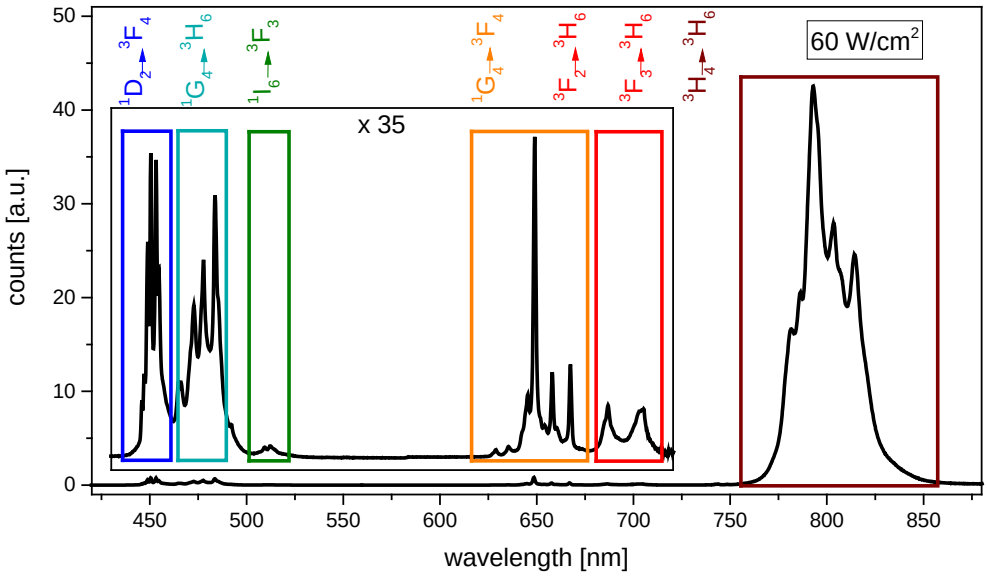

Figure S6. Upconversion emission spectra with color-encoded emission bands of the optical transitions $^1D_2 \rightarrow {}^3F_4$ (451 nm), $^1G_4 \rightarrow {}^3H_6$ (480 nm), $^1I_6 \rightarrow {}^3F_3$ (511 nm), $^1G_4 \rightarrow {}^3F_4$ (645 nm), $^3F_2 \rightarrow {}^3H_6$ (686 nm), $^3F_3 \rightarrow {}^3H_6$ (704 nm) and $^3H_4 \rightarrow {}^3H_6$ (794 nm), measured at P_{exc} = 60 W·cm^{-2}.

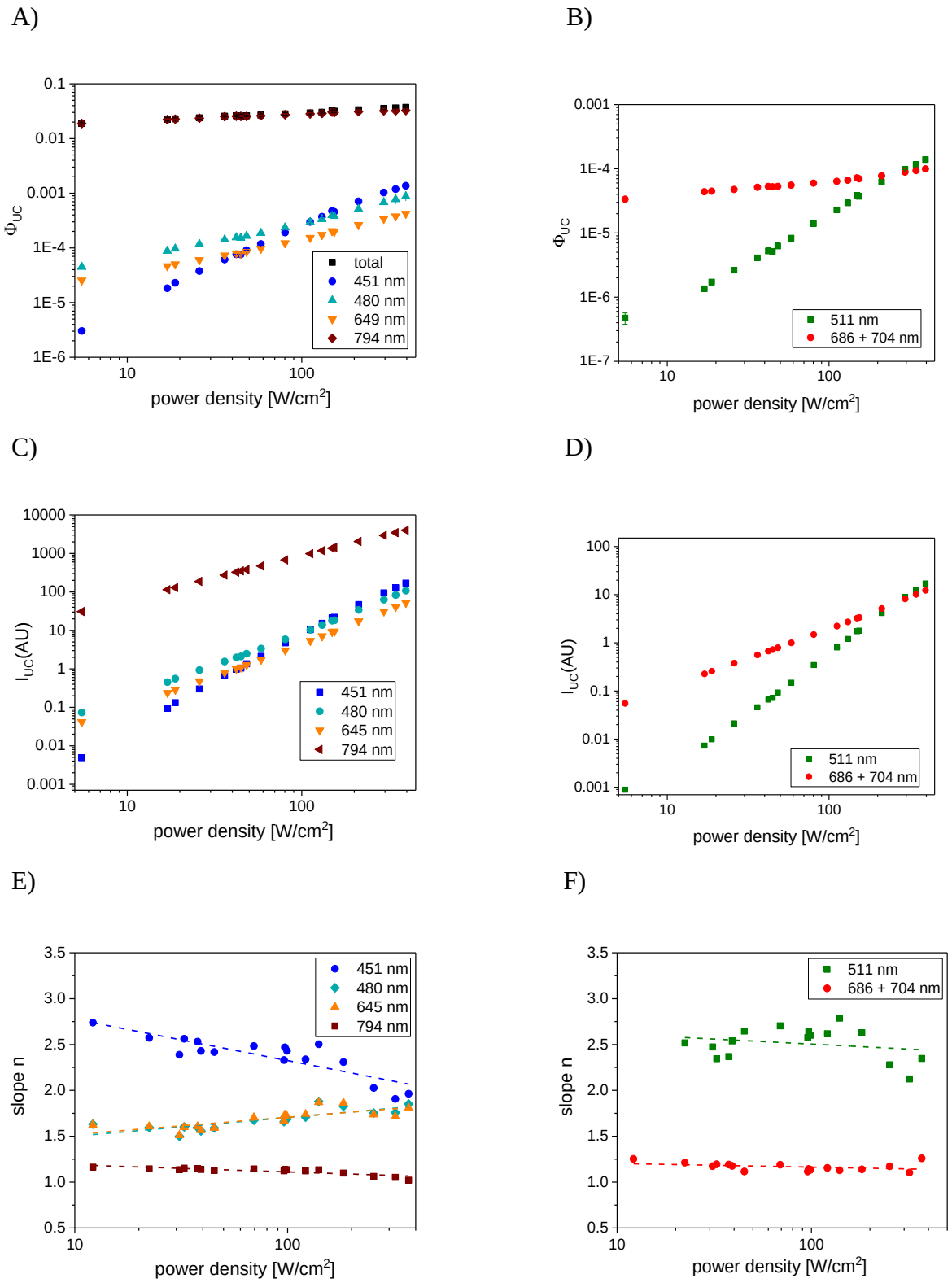

Figure S7. Panel A and B: Excitation power dependence of the absolute quantum yield Φ_{UC} of the major (A) and minor (B) emission bands. Panel C and D: power density dependent relative emitted intensities I_{UC} of the major (C) and minor (D) emission bands. Panel E and F: corresponding power density-dependent slope factors *n*.

8. Excitation power dependence of the upconversion quantum yield (comparison of data from all three groups)

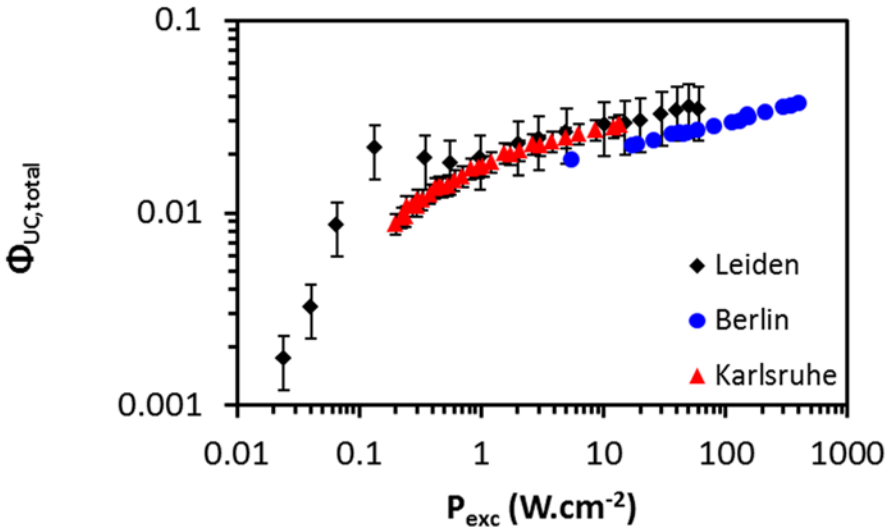

Figure S8. P_{exc} **dependence of** $\Phi_{UC,total}$ **of** $LiYF_4:Yb^{3+},Tm^{3+}$ **UCNPs in toluene, measured in Leiden (black diamonds), Berlin (blue circles), and Karlsruhe (red triangles).**

Table S1. Upconversion photoluminescence quantum yields ($\Phi_{UC,\lambda}$) for $LiYF_4:Yb^{3+},Tm^{3+}$ UCNPs in toluene. The data points from Leiden were measured relative to the value at 5.0 W·cm^{-2} at 293 K.

	P_{exc} [W.cm^{-2}]	$\Phi_{UC,451}$	$\Phi_{UC,480}$	$\Phi_{UC,511}$	$\Phi_{UC,649}$	$\Phi_{UC,686+704}$	$\Phi_{UC,794}$	$\Phi_{UC,total}$
Leiden [a]	0.024	n.d.	n.d.	n.d.	n.d.	n.d.	$1.8(5) \times 10^{-3}$	$1.8(5) \times 10^{-3}$
	0.04	n.d.	n.d.	n.d.	n.d.	n.d.	$3.2(10) \times 10^{-3}$	$3.2(10) \times 10^{-3}$
	0.07	n.d.	n.d.	n.d.	n.d.	n.d.	$9(3) \times 10^{-3}$	$9(3) \times 10^{-3}$
	0.13	n.d.	$7(2) \times 10^{-6}$	n.d.	n.d.	n.d.	0.021(7)	0.021(7)
	0.35	n.d.	$1.2(4) \times 10^{-5}$	n.d.	$8(3) \times 10^{-6}$	$2.0(6) \times 10^{-5}$	0.019(6)	0.019(6)
	0.56	$4(1) \times 10^{-7}$	$1.5(5) \times 10^{-5}$	n.d.	$9(3) \times 10^{-6}$	$2.4(7) \times 10^{-5}$	0.018(6)	0.018(6)
	0.98	$6(2) \times 10^{-7}$	$2.1(7) \times 10^{-5}$	n.d.	$1.1(3) \times 10^{-5}$	$2.4(8) \times 10^{-5}$	0.019(6)	0.019(6)
	2.0	$2.0(6) \times 10^{-6}$	$4(1) \times 10^{-5}$	n.d.	$1.8(6) \times 10^{-5}$	$2.7(9) \times 10^{-5}$	0.023(7)	0.023(7)
	3.0	$3(1) \times 10^{-6}$	$5(2) \times 10^{-5}$	n.d.	$2.3(7) \times 10^{-5}$	$3.0(9) \times 10^{-5}$	0.024(8)	0.024(8)
	5.0	$7(2) \times 10^{-6}$	$7(2) \times 10^{-5}$	$5(2) \times 10^{-7}$	$3.3(10) \times 10^{-5}$	$3.5(11) \times 10^{-5}$	0.026(8)	0.026(8)
	10	$2.2(7) \times 10^{-5}$	$1.0(3) \times 10^{-4}$	$1.0(3) \times 10^{-6}$	$5(2) \times 10^{-5}$	$4.1(13) \times 10^{-5}$	0.028(9)	0.029(9)
	15	$3.2(10) \times 10^{-5}$	$1.2(4) \times 10^{-4}$	$1.4(4) \times 10^{-6}$	$6(2) \times 10^{-5}$	$4.2(13) \times 10^{-5}$	0.029(9)	0.029(9)
	20	$5(2) \times 10^{-5}$	$1.4(5) \times 10^{-4}$	$3(1) \times 10^{-6}$	$7(2) \times 10^{-5}$	$4.3(14) \times 10^{-5}$	0.030(9)	0.030(9)
	30	$1.0(3) \times 10^{-4}$	$1.9(6) \times 10^{-4}$	$7(2) \times 10^{-6}$	$9(3) \times 10^{-5}$	$4.9(16) \times 10^{-5}$	0.032(10)	0.032(10)
	40	$1.6(5) \times 10^{-4}$	$2.5(8) \times 10^{-4}$	$1.1(3) \times 10^{-5}$	$1.2(4) \times 10^{-4}$	$5.4(17) \times 10^{-5}$	0.034(11)	0.034(11)
	50	$2.3(7) \times 10^{-4}$	$2.8(9) \times 10^{-4}$	$1.6(5) \times 10^{-5}$	$1.4(4) \times 10^{-4}$	$5.7(18) \times 10^{-5}$	0.035(11)	0.035(11)
	60	$2.4(8) \times 10^{-4}$	$2.9(9) \times 10^{-4}$	$1.7(5) \times 10^{-5}$	$1.4(4) \times 10^{-4}$	$5.6(18) \times 10^{-5}$	0.034(11)	0.034(11)
Karlsruhe [b]	0.20	n.d.	n.d.	n.d.	n.d.	n.d.	$9(1) \times 10^{-3}$	$9(1) \times 10^{-3}$
	0.27	n.d.	n.d.	n.d.	n.d.	n.d.	0.011(1)	0.011(1)
	0.33	n.d.	n.d.	n.d.	n.d.	n.d.	0.012(1)	0.012(1)
	0.38	n.d.	n.d.	n.d.	n.d.	n.d.	0.013(2)	0.013(2)
	0.48	n.d.	n.d.	n.d.	n.d.	n.d.	0.014(2)	0.014(2)
	0.54	n.d.	n.d.	n.d.	n.d.	n.d.	0.014(2)	0.014(2)
	0.61	n.d.	n.d.	n.d.	n.d.	n.d.	0.015(2)	0.015(2)
	0.70	n.d.	n.d.	n.d.	n.d.	n.d.	0.016(2)	0.016(2)
	0.95	n.d.	n.d.	n.d.	n.d.	n.d.	0.017(2)	0.017(2)
	1.04	n.d.	n.d.	n.d.	n.d.	n.d.	0.018(2)	0.018(2)
	1.21	n.d.	n.d.	n.d.	n.d.	n.d.	0.019(2)	0.019(2)
	1.54	n.d.	n.d.	n.d.	n.d.	n.d.	0.020(2)	0.020(2)
	2.1	n.d.	n.d.	n.d.	n.d.	n.d.	0.021(3)	0.021(3)
	2.6	n.d.	n.d.	n.d.	n.d.	n.d.	0.023(3)	0.023(3)
	3.1	n.d.	n.d.	n.d.	n.d.	n.d.	0.022(3)	0.022(3)
	3.8	n.d.	$5.0(16) \times 10^{-5}$	n.d.	n.d.	n.d.	0.023(3)	0.023(3)
	5.0	$1.6(10) \times 10^{-5}$	$6.3(18) \times 10^{-5}$	n.d.	n.d.	n.d.	0.025(3)	0.025(3)
	6.3	$2.1(11) \times 10^{-5}$	$7.4(18) \times 10^{-5}$	n.d.	$3.3(20) \times 10^{-5}$	n.d.	0.026(3)	0.026(3)
	8.7	n.d.	n.d.	n.d.	n.d.	n.d.	0.027(3)	0.027(3)
	12.1	$3.5(16) \times 10^{-5}$	$1.1(2) \times 10^{-4}$	n.d.	$5.3(24) \times 10^{-5}$	n.d.	0.028(3)	0.028(3)
	13.5	$4.5(14) \times 10^{-5}$	$1.2(2) \times 10^{-4}$	n.d.	$6.77(19) \times 10^{-5}$	n.d.	0.029(3)	0.029(3)
Berlin [c]	5.5	3.02×10^{-6}	$4.48(2) \times 10^{-5}$	$4.7(9) \times 10^{-7}$	$2.54(3) \times 10^{-5}$	$3.356(9) \times 10^{-5}$	0.0188	0.0189(5)
	17	$1.83(1) \times 10^{-5}$	$8.80(3) \times 10^{-5}$	1.4×10^{-6}	$4.64(1) \times 10^{-5}$	$4.39(1) \times 10^{-5}$	0.0222	0.022(2)
	19	$2.30(1) \times 10^{-5}$	$9.68(1) \times 10^{-5}$	$1.7(1) \times 10^{-6}$	$5.03(1) \times 10^{-5}$	$4.48(1) \times 10^{-5}$	0.0226	0.023(1)
	26	$3.78(2) \times 10^{-5}$	$1.168(4) \times 10^{-4}$	2.6×10^{-6}	$6.01(1) \times 10^{-5}$	4.8×10^{-5}	0.0236	0.024(1)
	36	$6.12(1) \times 10^{-5}$	$1.42(1) \times 10^{-4}$	4.1×10^{-6}	$7.31(5) \times 10^{-5}$	$5.15(1) \times 10^{-5}$	0.0251	0.0256(8)
	42	$7.65(1) \times 10^{-5}$	$1.55(1) \times 10^{-4}$	5.2×10^{-6}	$7.99(7) \times 10^{-5}$	$5.29(1) \times 10^{-5}$	0.0256	0.0261(8)
	45	$7.59(6) \times 10^{-5}$	$1.52(2) \times 10^{-4}$	5.2×10^{-6}	$7.88(8) \times 10^{-5}$	$5.23(1) \times 10^{-5}$	0.0254	0.026(2)
	48	$9.08(5) \times 10^{-5}$	$1.65(1) \times 10^{-4}$	6.2×10^{-6}	$8.48(5) \times 10^{-5}$	5.3×10^{-5}	0.0255	0.0260(6)
	58	$1.177(1) \times 10^{-4}$	$1.86(1) \times 10^{-4}$	8.3×10^{-6}	$9.67(5) \times 10^{-5}$	5.5×10^{-5}	0.0261	0.027(1)
	80	$1.913(3) \times 10^{-4}$	$2.36(1) \times 10^{-4}$	$1.40(1) \times 10^{-5}$	$1.224(6) \times 10^{-4}$	$5.97(1) \times 10^{-5}$	0.0273	0.028(1)
	112	$2.987(3) \times 10^{-4}$	$2.96(2) \times 10^{-4}$	$2.29(1) \times 10^{-5}$	$1.53(1) \times 10^{-4}$	$6.37(3) \times 10^{-5}$	0.0283	0.029(1)
	131	$3.713(3) \times 10^{-4}$	$3.35(2) \times 10^{-4}$	2.9×10^{-5}	$1.73(1) \times 10^{-4}$	$6.63(3) \times 10^{-5}$	0.0288	0.030(1)
	149	$4.75(1) \times 10^{-4}$	$3.96(3) \times 10^{-4}$	$3.86(2) \times 10^{-5}$	$2.04(1) \times 10^{-4}$	$7.22(2) \times 10^{-5}$	0.0305	0.0323(2)
	154	$4.57(2) \times 10^{-4}$	$3.81(2) \times 10^{-4}$	$3.72(2) \times 10^{-5}$	$1.962(7) \times 10^{-4}$	$6.98(2) \times 10^{-5}$	0.0299	0.032(2)
	212	7.12×10^{-4}	$5.15(3) \times 10^{-4}$	6.3×10^{-5}	$2.631(8) \times 10^{-4}$	$7.8(1) \times 10^{-5}$	0.0310	0.034(2)
	295	1.03×10^{-3}	$6.84(3) \times 10^{-4}$	$9.74(2) \times 10^{-5}$	$3.406(9) \times 10^{-4}$	$8.89(2) \times 10^{-5}$	0.0321	0.036(2)
	345	1.19×10^{-3}	$7.729(7) \times 10^{-4}$	$1.166(9) \times 10^{-4}$	$3.790(9) \times 10^{-4}$	$9.37(2) \times 10^{-5}$	0.0322	0.0363(5)
	395	1.37×10^{-3}	$8.78(2) \times 10^{-4}$	$1.390(6) \times 10^{-4}$	$4.24(1) \times 10^{-4}$	$9.97(2) \times 10^{-5}$	0.0325	0.0371(7)

[a] λ_{exc} = 969 nm; [b] λ_{exc} = 980 nm; [c] λ_{exc} = 976 nm; n.d.: not determined.

9. Excitation wavelength dependence of the upconversion emission intensity (Karlsruhe)

The luminescence excitation spectra of the dispersed UCNPs were measured with a home-built setup. Continuous-wave (CW) tunable Ti-Sapphire laser (Solstis, M squared) was used as an excitation source. During a wavelength sweep the P_{exc} on the front surface of the sample was measured (PM100D with S121C head, Thorlabs Inc.) and used afterwards for the correction of the excitation spectrum. The luminescence was collected by an optical fiber and directed to a calibrated CCD spectrometer (AvaSpec-ULS2048, Avantes). A dichroic filter (FES0750, Thorlabs Inc.) was placed in front of the collecting edge of the optical fiber in order to block the scattered excitation radiation. For each excitation wavelength the emission was integrated from 440 to 500 nm for the blue emission and from 750 to 850 nm for the NIR emission, respectively. The spectra were normalized in such a way that similar P_{exc} (~5 W·cm^{-2}) is used for each excitation wavelength. For simplicity, we assume that at the given range of the excitation power density (1.0 – 10 W·cm^{-2}) the power coefficient n (in $I_{UC} \sim P_{exc}^{n}$) is constant with n = 1.1 for 794 nm emission and n = 1.6 for 480 nm emission in agreement with Figure S4. Since the optical output power of our laser varies slightly (see Figure S9) over this wavelength range, the raw data were corrected according to $I_{UC(corrected)} \sim I_{UC(measured)}/(P_{exc/5})^{n}$, followed by normalization of the spectra.

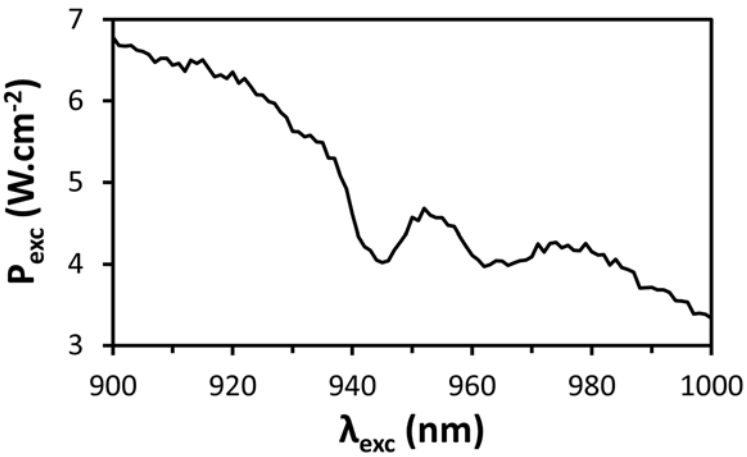

Figure S9. Optical output power density as a function of excitation wavelength for the laser system used for excitation wavelength dependence measurements in Karlsruhe.

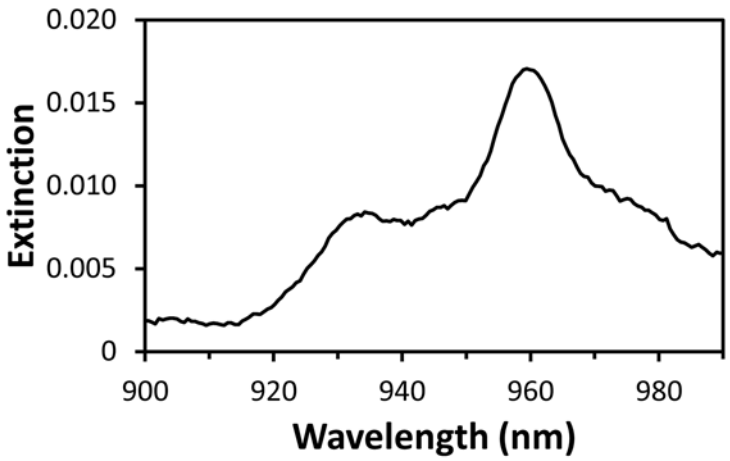

Figure S10. NIR absorption spectrum of $LiYF_4:Yb^{3+},Tm^{3+}$ UCNPs in toluene ([UCNP] = 10 mg·ml^{-1}) measured in Leiden.

10. Temperature dependence of the upconversion quantum yield (Leiden)

As integrating sphere setups do not feature temperature control, Φ_{UC} at other temperatures than 293 K was estimated from measuring the upconverted emission in the temperature-controlled cuvette holder setup (see Section 4) at a range of temperatures from 278 to 333 K and scaling Φ_{UC} at 293 K with the ratio of the upconversion emission at 293 K and the temperature of interest (T) by using Equation S12:

$$\Phi_{UC}^{T} = \Phi_{UC}^{293\,K} * \frac{\int_{\lambda_1}^{\lambda_2} I_{UC}^{T}(\lambda)d\lambda}{\int_{\lambda_1}^{\lambda_2} I_{UC}^{293\,K}(\lambda)d\lambda} \qquad \textbf{Equation S12}$$

For these measurements, 1.8 mL of a 5 mg·mL^{-1} of $LiYF_4$:Yb,Tm UCNPs dispersion in toluene were placed in a stirred 111-QS macro fluorescence cuvette (Hellma). The cuvette was placed in the temperature-controlled cuvette holder, and cooled to 278 K. After equilibrating for 10 minutes, the temperature was increased from 278 to 333 K with a rate of 1 K·min^{-1}, while recording the upconverted emission spectra. During the experiment, the temperature of the dispersion was monitored using a K-type probe submerged in the sample, and recorded on an Omega RDXL4SD thermometer. Integration of the emission bands was performed by fitting the emission bands with one or more Gaussian profiles, and integrating the area under these peaks. This treatment allowed deconvolution of the various emission bands, even though the emission data could only be recorded with a spectral resolution of 9 nm (slit size = 200 μm).

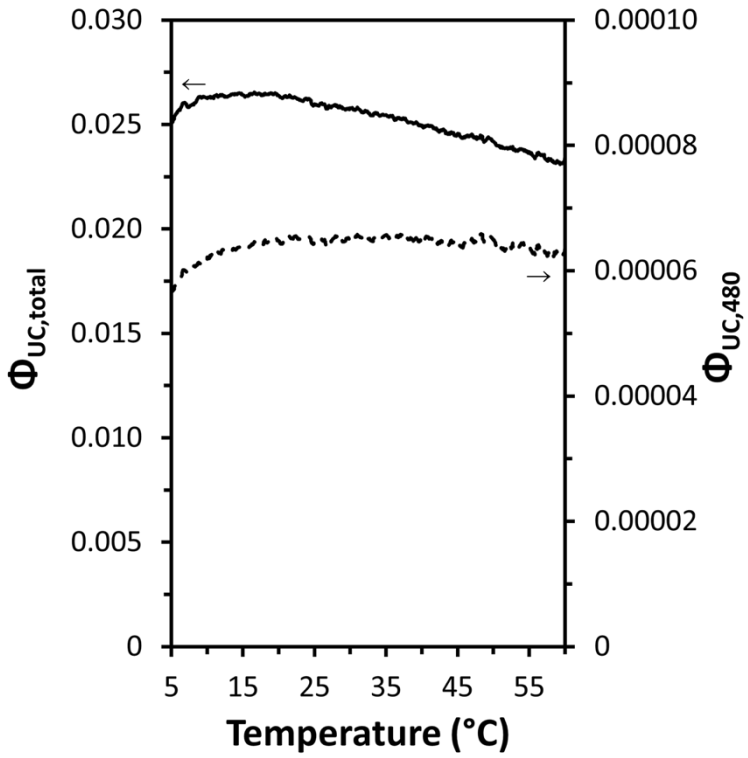

Figure S11. Temperature dependence of the total upconversion quantum yield $\Phi_{UC,total}$ (solid line, left axis) and of the upconversion quantum yield of the blue 480 nm band $\Phi_{UC,480}$ (dashed line, right axis) of $LiYF_4:Yb^{3+},Tm^{3+}$ UCNPs in toluene recorded in Leiden; λ_{exc} = 969 nm, P_{exc} = 5.0 W·cm^{-2}, [UCNP] = 5 mg·mL^{-1}.

Table S2. Temperature dependence of the upconversion quantum yield of $LiYF_4:Yb^{3+},Tm^{3+}$ UCNPs in toluene recorded in Leiden; λ_{exc} = 969 nm, [UCNP] = 5 mg·mL^{-1}.

T [°C]	$\Phi_{UC,451}$	$\Phi_{UC,480}$	$\Phi_{UC,649}$	$\Phi_{UC,686}$	$\Phi_{UC,704}$	$\Phi_{UC,794}$	$\Phi_{UC,total}$
10	6.4×10^{-6}	6.2×10^{-5}	3.0×10^{-5}	1.5×10^{-5}	2.1×10^{-5}	0.026	0.026
20	6.4×10^{-6}	6.5×10^{-5}	3.1×10^{-5}	1.5×10^{-5}	2.1×10^{-5}	0.026	0.026
37	6.4×10^{-6}	6.6×10^{-5}	3.0×10^{-5}	1.6×10^{-5}	2.2×10^{-5}	0.025	0.025
50	6.2×10^{-6}	6.5×10^{-5}	3.0×10^{-5}	1.7×10^{-5}	2.3×10^{-5}	0.024	0.024

11. Luminescence lifetime measurements (Karlsruhe)

For the photoluminescence lifetime measurements, time-correlated single photon counting TCSPC and a multichannel scaling (MCS) card (Timeharp 260, PicoQuant) were used. The modulation of the diode laser was performed via a built-in function generator in the laser diode driver. In order to detect the rise and decay times of the emission, the TTL signal from the laser diode controller was delayed by the use of a delay generator (DG645, Stanford Research Systems). The spectral separation of the photoluminescence was achieved via a double monochromator (DTMS300, Bentham) and the emission at 998 nm was detected via a cooled InGaAs/InP avalanche photodiode ID220-FR (ID Quantique SA). The sample was excited with a 940 nm laser diode using 15 ms long pulses followed by a 20 ms dark time. These pulses are of sufficient length to drive the population processes into the steady state during the time in which the laser is on. After the laser is turned off we monitor how the downconverted luminescence of Yb^{3+} decays with time.

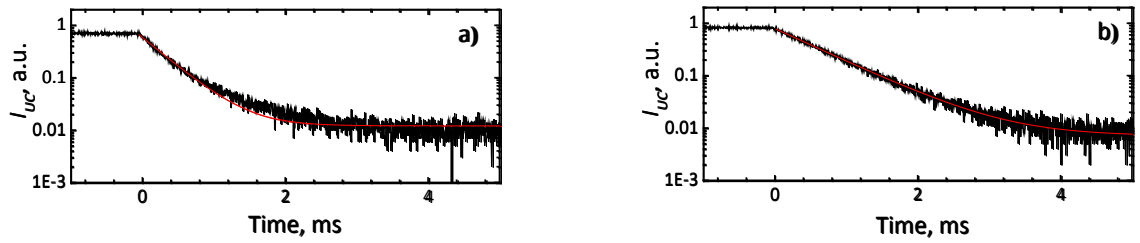

Figure S12. Luminescence decays of $LiYF_4:Yb^{3+},Tm^{3+}$ UCNPs excited at 940 nm for the Yb^{3+}: $^2F_{5/2}\rightarrow{}^2F_{7/2}$ emission, detected at 998 nm; P_{exc} = 220 W·cm^{-2} (a) and 10 W·cm^{-2} (b). Red lines are the single exponential fits. Data obtained in Karlsruhe.

References

1. P. A. Rojas-Gutierrez, C. DeWolf and J. A. Capobianco, *Part. Part. Syst. Charact.*, 2016, **33**, 865-870.
2. V. Mahalingam, F. Vetrone, R. Naccache, A. Speghini and J. A. Capobianco, *Adv. Mater.*, 2009, **21**, 4025-4028.
3. J. C. de Mello, H. F. Wittmann and R. H. Friend, *Adv. Mater.*, 1997, **9**, 230-232.
4. D. O. Faulkner, J. J. McDowell, A. J. Price, D. D. Perovic, N. P. Kherani and G. A. Ozin, *Laser Photonics Rev.*, 2012, **6**, 802-806.
5. M. Kaiser, C. Würth, M. Kraft, I. Hyppanen, T. Soukka and U. Resch-Genger, *Nanoscale*, 2017, **9**, 10051-10058.
6. C. Würth, J. Pauli, C. Lochmann, M. Spieles and U. Resch-Genger, *Anal. Chem.*, 2012, **84**, 1345-1352.
7. C. Würth, M. Grabolle, J. Pauli, M. Spieles and U. Resch-Genger, *Anal. Chem.*, 2011, **83**, 3431-3439.
8. S. Hatami, C. Würth, M. Kaiser, S. Leubner, S. Gabriel, L. Bahrig, V. Lesnyak, J. Pauli, N. Gaponik, A. Eychmuller and U. Resch-Genger, *Nanoscale*, 2015, **7**, 133-143.
9. U. Resch-Genger, W. Bremser, D. Pfeifer, M. Spieles, A. Hoffmann, P. C. DeRose, J. C. Zwinkels, F. Gauthier, B. Ebert, R. D. Taubert, C. Monte, J. Voigt, J. Hollandt and R. Macdonald, *Anal. Chem.*, 2012, **84**, 3889-3898.